

Common Features in Electronic Structure of the Fe-Based Layered Superconductors from Photoemission Spectroscopy

Xiaowen Jia¹, Haiyun Liu¹, Wentao Zhang¹, Lin Zhao¹, Jianqiao Meng¹, Guodong Liu¹, Xiaoli Dong¹, G. F. Chen¹, J. L. Luo¹, N. L. Wang¹, Z. A. Ren¹, Wei Yi¹, Jie Yang¹, Wei Lu¹, G. C. Che¹, G. Wu², R. H. Liu², X. H. Chen², Guiling Wang¹, Yong Zhou¹, Yong Zhu³, Xiaoyang Wang³, Zhongxian Zhao¹, Zuyan Xu¹, Chuangtian Chen³, X. J. Zhou^{1,*}

¹Beijing National Laboratory for Condensed Matter Physics,

Institute of Physics, Chinese Academy of Sciences, Beijing 100190, China

²Hefei National Laboratory for Physical Sciences at Microscale and Department of Physics,

University of Science and Technology of China, Hefei, Anhui 230026, China

³Technical Institute of Physics and Chemistry, Chinese Academy of Sciences, Beijing 100190, China

(Dated: June 2, 2008)

High resolution photoemission measurements have been carried out on non-superconducting LaOFeAs parent compound and various superconducting $R(O_{1-x}F_x)FeAs$ ($R=La, Ce$ and Pr) compounds. We found that the parent LaOFeAs compound shows a metallic character. Through extensive measurements, we have identified several common features in the electronic structure of these Fe-based compounds: (1). 0.2 eV feature in the valence band; (2). A universal 13~16 meV feature; (3). A clear Fermi cutoff showing zero leading-edge shift in the superconducting state; (4). Lack of superconducting coherence peak(s); (5). Near E_F spectral weight suppression with decreasing temperature. These universal features can provide important information about band structure, superconducting gap and pseudogap in these Fe-based materials.

PACS numbers: 74.70.-b, 74.25.Jb, 79.60.-i, 71.20.-b

The discovery of superconductivity in Fe-based oxypnictides[1, 2, 3, 4, 5, 6, 7, 8, 9] has generated a great interest because it represents the second class of “high temperature superconductors” after the first one in the cuprates[10]. The parent compound of these Fe-based superconductors has been found to exhibit a spin density wave(SDW)-like transition near 150 K and a possible antiferromagnetic ground state[9, 11, 12, 13]. Doping charge carriers into the system induces superconductivity at appropriate doping levels. These behaviors appear to be similar to those in cuprate superconductors. Some important questions to ask include: (1). Whether these materials can be categorized into strong correlated electron systems; (2). Whether the mechanism of superconductivity is conventional or exotic; (3). Whether the normal state is anomalous or whether there is a pseudogap in the normal state as found in the cuprate superconductors[14]. Photoemission spectroscopy, as a powerful tool to directly measure the electronic structure and energy gap, can shed important light on these issues[15, 16, 17, 18, 19].

In this paper, we report high resolution photoemission measurements on various $R(O_{1-x}F_x)FeAs$ compounds ($R=La, Ce$ and Pr). We have found that the parent LaOFeAs compound shows a metallic behavior which is distinct from the antiferromagnetic insulator in the parent compound of cuprate superconductors. Through extensive measurements, we have identified several common features in the electronic structure of the Fe-based compounds: (1). 0.2 eV feature in the valence band; (2). A universal 13~16 meV feature; (3). A clear Fermi cutoff

showing zero leading-edge shift in the superconducting state; (4). Lack of superconducting coherence peak(s); (5). Near E_F spectral weight suppression with decreasing temperature. These universal features can provide important information about band structure, superconducting gap and pseudogap in these Fe-based compounds.

The photoemission measurements have been carried out on our newly-developed system using both Vacuum Ultraviolet (VUV) laser and Helium discharge lamp as light sources, equipped with Scienta R4000 electron energy analyzer[19, 20]. The laser photon energy ($h\nu$) is 6.994 eV and the spot size is less than 0.2 mm. For the laser measurements, the energy resolution was set at 1.0 meV. The Helium lamp can provide two photon energies at 21.218 eV (Helium I resonance line) and 40.813 eV (Helium II resonance line). The energy resolution for the 21.218 eV and 40.813 eV valence band measurements was set at 12.5~20 meV. Polycrystalline $R(O_{1-x}F_x)FeAs$ ($R=La, Ce$ and Pr) samples with various dopings (x , nominal composition) are prepared by solid state reaction method[5, 7, 11]. The LaOFeAs sample is not superconducting but with a possible SDW transition at ~ 150 K[11], while the $LaO_{0.92}F_{0.08}FeAs$, $CeO_{0.88}F_{0.12}FeAs$ and $PrO_{0.89}F_{0.11}FeAs$ samples are superconducting with T_c at 26 K, 38 K and 48 K, respectively[5, 7, 11]. To get clean surface and avoid sample aging effect[19], all the laser photoemission data presented in the work were measured on a fresh sample surface within 3~4 hours after *in situ* fracturing in vacuum with a base pressure better than 5×10^{-11} Torr.

Fig. 1 shows photoemission spectra of $R(O_{1-x}F_x)FeAs$

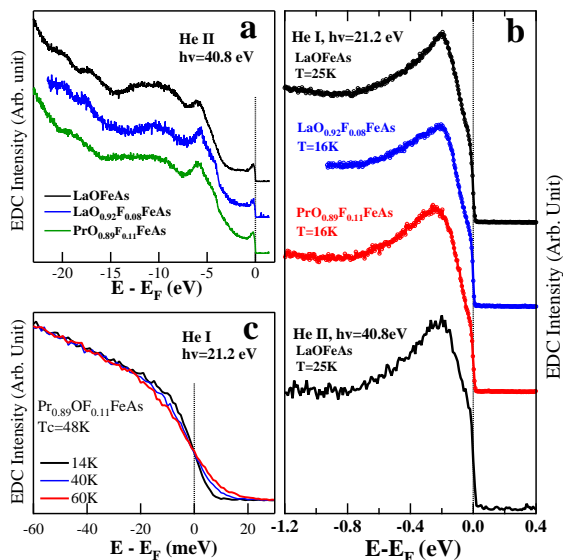


FIG. 1: Photoemission spectra of $R(O_{1-x}F_x)FeAs$ ($R=La$ and Pr) samples measured using 21.2 eV and 40.8 eV photon energies from the Helium lamp. (a). Large energy range photoemission spectra of $LaOFeAs$, $LaO_{0.92}F_{0.08}FeAs$ and $PrO_{0.89}F_{0.11}FeAs$ measured using 40.8 eV photon energy from Helium lamp. (b). Valence band of $LaOFeAs$, $LaO_{0.92}F_{0.08}FeAs$ and $PrO_{0.89}F_{0.11}FeAs$ measured using 21.2 eV and 40.8 eV photon energies from Helium lamp. (3). Temperature dependence of near- E_F spectra for the $PrO_{0.89}F_{0.11}FeAs$ sample measured using 21.2 eV photon energy with an energy resolution of 6.5 meV.

($R=La$ and Pr) samples measured using different photon energies of the Helium lamp. Over a large energy range (Fig. 1a), these samples show similar photoemission spectra with two main peaks near 0.2 eV and ~ 6 eV, one broad feature between $7\sim 14$ eV, and some weak peaks at higher binding energy[16, 18, 21]. The valence band shows mainly a pronounced peak at 0.2 eV (Fig. 1b). Different photon energies give similar spectra as seen from the 21.2 eV and 40.8 eV measurements on the $LaOFeAs$ sample. Different samples show similar spectra and there is no dramatic spectral change between the undoped $LaOFeAs$ and doped $LaO_{0.92}F_{0.08}FeAs$ samples. Particularly, the parent $LaOFeAs$ compound shows a clear Fermi cutoff (Figs. 1 and 2), indicating its metallic nature. This is distinct from the cuprates where the parent compound is an antiferromagnetic insulator[15].

Fig. 2 shows photoemission spectra of $R(O_{1-x}F_x)FeAs$ ($R=La, Ce$ and Pr) measured using laser at 14 K. The $LaOFeAs$ parent compound and the superconducting samples exhibit similar low energy spectra where two obvious kink features can be identified. One is at higher binding energy where the spectrum starts to deviate from the linear behavior, ~ 16 meV for $LaOFeAs$ and $LaO_{0.92}F_{0.08}FeAs$ and ~ 13 meV for $CeO_{0.88}F_{0.12}FeAs$ and $PrO_{0.89}F_{0.11}FeAs$ [22]. The other is at lower bind-

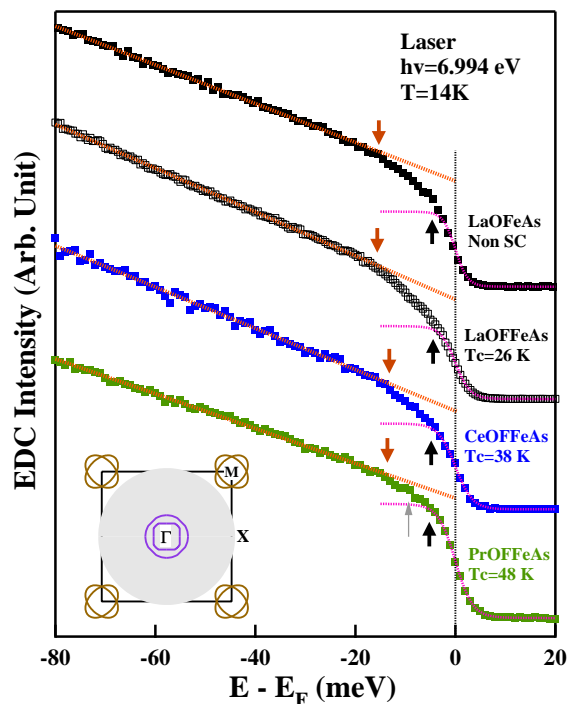


FIG. 2: Photoemission spectra of $LaOFeAs$, $LaO_{0.92}F_{0.08}FeAs$, $CeO_{0.88}F_{0.12}FeAs$ and $PrO_{0.89}F_{0.11}FeAs$ samples taken with laser (6.994 eV) at 14 K. The high binding energy part between 20 and 80 meV shows linear behavior, as indicated by the fitted dashed lines. The curves start to deviate from the linear line at 13~16 meV, as indicated by the down arrows. Upon approaching the Fermi level, another drop occurs at ~ 4 meV, as marked by the black up arrows. The spectra near the Fermi level can be well fitted using Fermi-Dirac distribution function, as indicated by the purple dotted curves. The inset shows a schematic Brillouin zone and the calculated Fermi surface[11, 25]. The momentum area that can be covered by angle-integrated laser photoemission is marked as a shaded region.

ing energy near 4 meV that is due to the Fermi function cutoff. The $13\sim 16$ meV feature is robust because it is present in both undoped sample and doped samples, in different superconducting materials ($R=La, Ce, Pr$ and Sm [19]), and seen in both laser photoemission data and high resolution helium lamp measured data[19].

The high resolution low temperature data in Fig. 2 provide a good opportunity to examine the superconducting gap in these Fe-based superconductors. Generally speaking, in the momentum-integrated photoemission spectrum, it is straightforward to determine one superconducting gap on a single Fermi surface by following the leading-edge shift, as exemplified in superconducting diamond[23]. In a system with multiple superconducting gaps on different Fermi surface sheets, the leading edge position is mainly dictated by the minimum superconducting gap on a Fermi surface sheet; the larger energy gaps on the other Fermi surface sheets will show up

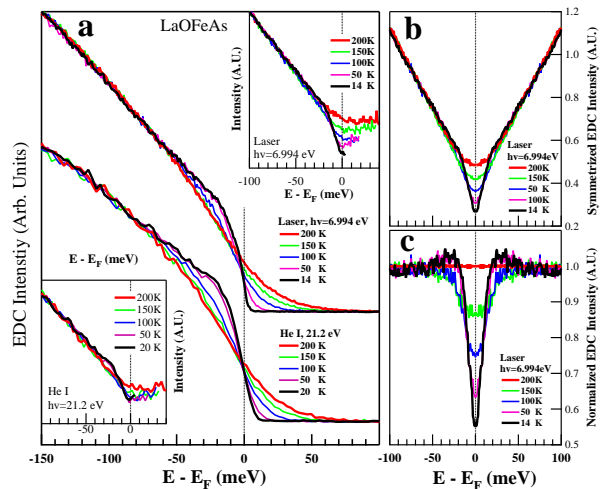


FIG. 3: (a). Temperature dependence of the photoemission spectra on the LaOFeAs sample measured by laser and 21.2 eV photon energy from the helium lamp. The upright and bottom-left insets show the laser data and helium lamp data, respectively, with the Fermi-Dirac distribution function removed. (b). Symmetrized spectra from laser data in (a) with respect to the Fermi level. (c). Symmetrized laser spectra divided by the data at 200 K. To avoid statistical noise, the 200 K data is fitted with a polynomial and used for the normalization.

as additional features in the spectrum at higher binding energy, as demonstrated in a two-gap system like MgB₂[24]. However, the situation may get complicated if a superconductor has multiple gaps involving unconventional pairing symmetry and/or does not show clear superconducting coherence peaks.

The Fe-based compounds exhibit unusual superconducting behaviors in two aspects. The first is the lack of superconducting coherence peaks in the measured photoemission spectra for all these R(O_{1-x}F_x)FeAs superconductors even though they have a rather high superconducting temperature at 26 K, 38 K, and 48 K for R=La, Ce and Pr, respectively (Fig. 2). This may be related to either strong disorder, or unconventional superconducting pairing in these samples. The second is the ubiquitous existence of a clear Fermi cutoff that shows little leading-edge shift in the superconducting state (Fig. 2). Since the Fe-based compounds have multiple hole-like Fermi surface sheets around Γ point and electron-like sheets around M(π , π) point (inset of Fig. 2)[11], they may have different superconducting order parameters among different Fermi surface sheets. If the clear Fermi cut-off is not due to non-superconducting metallic impurities in the samples, it indicates that there are un-gapped Fermi surface sheet(s) in the Fe-based superconductors. As the laser photoemission ($h\nu=6.994$ eV) can only cover the Fermi surface sheets around Γ point[25], but not those around the M(π , π) point (inset of Fig. 2),

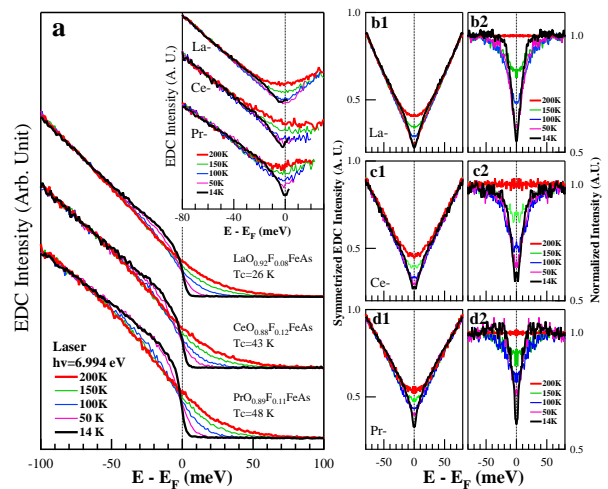


FIG. 4: (a). Temperature dependence of the laser photoemission spectra on the La(O_{0.92}F_{0.08})FeAs, CeO_{0.88}F_{0.12}FeAs and PrO_{0.89}F_{0.11}FeAs samples. The upright inset shows the corresponding data but with the Fermi-Dirac distribution function removed. (b1),(c1) and (d1) show symmetrized laser spectra from (a) with respect to the Fermi level. (b2),(c2) and (d2) show corresponding symmetrized spectra divided by the 200 K data. To avoid statistical noise, the 200 K data is fitted with a polynomial and used for the normalization.

these laser data may further suggest that there are un-gapped Fermi surface sheet(s) near the Γ point.

To identify superconducting gaps on all the Fermi surface sheets, one has to look for signatures in the momentum-integrated photoemission spectra at higher binding energies away from the Fermi cutoff. It is natural to see whether the 13~16 meV feature may represent a superconducting gap structure (Fig. 2). However, the observation of the same feature in undoped non-superconducting LaOFeAs and SmOFeAs[19] has unambiguously ruled out this possibility. No other clear features between the Fermi level and 13~16 meV can be identified from the laser data in LaO_{0.92}F_{0.08}FeAs and CeO_{0.88}F_{0.12}FeAs but there seems to be a feature near 9 meV in PrO_{0.89}F_{0.11}FeAs which needs to be further checked on its reproducibility with higher precision and data quality (Fig. 2). In order to be able to probe the superconducting gap on all the Fermi surface sheets including those near the M(π , π) point (inset of Fig. 2), we also took high resolution data on the PrO_{0.89}F_{0.11}FeAs superconductor at different temperatures using the Helium lamp (Fig. 1c). Like the laser data, there is no superconducting coherence peak(s) developed and there is a clear Fermi cut-off with nearly zero leading-edge shift below the superconducting temperature. For the same reason as in the laser case, one has to look for the signature of the superconducting gaps at higher binding energy but no signatures seem to be clearly identifiable in the data except for the 13~16 meV feature (inset of Fig.

1). We note that the difficulty to clearly identify superconducting gaps on all the Fermi surface sheets does not mean there are no superconducting gaps opening in these Fe-based superconductors. It indicates further measurements with better resolution and higher data statistics are needed to search for the subtle features in the photoemission spectra.

Fig. 3 shows detailed temperature dependence of the photoemission spectra for the undoped LaOFeAs sample measured using both laser and helium lamp. In both cases, the temperature-induced change is mainly confined near the Fermi level $[-70\text{meV}, 70\text{meV}]$ range; the high binding energy spectra at different temperatures can be normalized to overlap with each other. Note that the spectra at different temperatures do not cross the same point at the Fermi level, a behavior that is different from a normal metal like gold where all spectra cross at the same energy E_F . To remove the effect of thermal broadening effect, the spectra are divided by Fermi-Dirac distribution function at the respective temperature and shown in the insets of Fig. 3. There is a clear suppression of the spectral weight near the Fermi level with decreasing temperature in the laser data (upright inset of Fig. 3a), a behavior that starts at temperatures even as high as 150 K. The helium lamp data (bottom-left inset of Fig. 3a) are consistent with the laser data although the magnitude of near- E_F spectral weight suppression appears to be weaker. This spectral weight loss is similar to the normal state spectral weight depletion near the antinodal region in the underdoped cuprate superconductors which is related to the opening of a pseudogap[14].

To further examine the possible opening of the pseudogap in Fe-based compounds, we follow the procedure that is commonly used in high- T_c cuprate superconductors[26] by symmetrizing the original data in Fig. 3a with respect to the Fermi level (Fig. 3b). This is another way to remove the Fermi-Dirac distribution function and it provides a visualized way to look for a gap. Again one sees clearly the depletion of spectral weight near the Fermi level with decreasing temperature (Fig. 3b). To highlight the effect caused by temperature, we further divide the symmetrized spectra with the one at 200 K (Fig. 3c). The suppression of the spectral weight near the Fermi level becomes clearer and one can now identify an energy scale at which the spectral weight starts to lose. It is in the 25~40 meV energy range for different temperatures (Fig. 3c).

The temperature dependence of photoemission spectra for the superconducting samples (Fig. 4) appears to be surprisingly similar among different materials and to that in the undoped LaOFeAs sample (Fig. 3). Here again one sees suppression of spectral weight with decreasing temperature as in the inset of Fig. 4a, symmetrized data in Fig. 4b1, c1 and d1 and normalized data in Fig. 4b2, c2 and d2 for $\text{LaO}_{0.92}\text{F}_{0.08}\text{FeAs}$, $\text{CeO}_{0.88}\text{F}_{0.12}\text{FeAs}$ and $\text{PrO}_{0.89}\text{F}_{0.11}\text{FeAs}$ samples, respectively. We note that

our results on the $\text{LaO}_{0.92}\text{F}_{0.08}\text{FeAs}$ sample are rather different from that measured by Ishida et al.[17]. Particularly, we do not observe any signature of 0.1 eV pseudogap as claimed by them[17]. This difference may be caused by sample surface cleanness because we found that the 0.2 eV peak feature in our sample (Fig. 1) is much sharper than that in theirs[17]. For these superconducting samples with $T_c=26\sim 48$ K, one may wonder whether the near- E_F spectral weight suppression in the superconducting state, like the 13 K data in Fig. 4, compared with a normal state data at 50 K, can be taken as a signature of superconducting gap opening, as did by Sato et al.[18]. Noting that the same behavior also occurs in the non-superconducting LaOFeAs sample (Fig. 3), we believe this is not a reliable way in judging on a superconducting gap.

In summary, from our extensive high resolution photoemission measurements on the $\text{R}(\text{O}_{1-x}\text{F}_x)\text{FeAs}$ ($\text{R}=\text{La}, \text{Ce}$ and Pr) compounds, together with previous measurements on $\text{Sm}(\text{O}_{1-x}\text{F}_x)\text{FeAs}$ [19], we have identified several universal features in the electronic structure of the Fe-based compounds. These universal features can provide important information about band structure, superconducting gap and pseudogap in these Fe-based compounds. The parent LaOFeAs compound shows a metallic nature that is distinct from the parent compound of cuprate superconductors that is a Mott insulator. The origin of the 13~16 meV feature and whether it can be due to electron coupling with some collective excitations need to be further studied. The zero leading-edge shift in the spectra in the superconducting state suggests that the Fermi surface sheet(s) around the Γ point may not be gapped. The spectral weight suppression near E_F with decreasing temperature points to possible existence of a pseudogap in the Fe-based compounds. Its origin as to whether it can be caused by local SDW fluctuation or strong electron-boson coupling needs further experimental and theoretical studies.

This work is supported by the NSFC, the MOST of China (973 project No: 2006CB601002, 2006CB921302), and CAS (Projects ITSNEM).

*Corresponding author: XJZhou@aphy.iphy.ac.cn

-
- [1] Y. Kamihara et al., *J. Am. Chem. Soc.* **130**, 3296 (2008).
 - [2] G. F. Chen et al., arXiv:cod-mat/0803.0128.
 - [3] H. H. Wen et al., *Europhys. Lett.* **82**, 17009 (2008).
 - [4] X. H. Chen et al., arXiv:cod-mat/0803.3603.
 - [5] G. F. Chen et al., arXiv:cod-mat/0803.3790.
 - [6] Z. A. Ren et al., *Europhys. Lett.* **82**, 57002 (2008).
 - [7] Z. A. Ren et al., arXiv:cod-mat/0803.4283.
 - [8] Z. A. Ren et al., *Chin. Phys. Lett.* **25**, 2215 (2008).
 - [9] R. H. Liu et al., arXiv:cond-mat/0804.2105.
 - [10] J. G. Bednorz et al., *Z. Phys. B* **64**, 189 (1986).
 - [11] J. Dong et al., arXiv:cond-mat/0803.3426.

- [12] C. Cruz et al., arXiv:cond-mat/0804.0795.
- [13] M. A. McGuire et al., arXiv:cond-mat/0804.0796.
- [14] T. Timusk and B. Statt, Rep. Prog. Phys. **62**, 61(1999).
- [15] A. Damascelli et al., Rev. Mod. Phys. **75**, 473(2003).
- [16] H. W. Ou et al., arXiv:cond-mat/0803.4328.
- [17] Y. Ishida et al., arXiv:cond-mat/0805.2647.
- [18] T. Sato et al., arXiv:cond-mat/0805.3001.
- [19] H. Y. Liu et al., arXiv:cond-mat/0805.
- [20] G. D Liu et al., Rev. Sci. Instruments **79**, 023105 (2008).
- [21] Because of the relatively large spot size of the helium lamp light, the high binding energy spectra may contain weak signals from graphite surrounding the sample, but the low binding energy part within 1 eV is not affected.
- [22] The uncertainty of the position determination is ± 3 meV.
- [23] K. Ishizaka et al., Phys. Rev. Lett. **98**, 047003 (2007).
- [24] S. Tsuda et al., Phys. Rev. B **72**, 064527 (2005).
- [25] The work function is assumed to be 4.3 eV.
- [26] M. R. Norman et al., Phys. Rev. B **57**, R11093 (1998).